

# Biallelic Mutations in *ADPRHL2*, Encoding ADP-Ribosylhydrolase 3, Lead to a Degenerative Pediatric Stress-Induced Epileptic Ataxia Syndrome

Shereen G. Ghosh,<sup>1,2</sup> Kerstin Becker,<sup>3,4,5</sup> He Huang,<sup>6,7</sup> Tracy D. Salazar,<sup>1,2</sup> Guoliang Chai,<sup>1,2</sup> Vincenzo Salpietro,<sup>8</sup> Lihadh Al-Gazali,<sup>9</sup> Quinten Waisfisz,<sup>10</sup> Haicui Wang,<sup>3,4,5</sup> Keith K. Vaux,<sup>11</sup> Valentina Stanley,<sup>1,2</sup> Andreea Manole,<sup>8</sup> Ugur Akpulat,<sup>3,4,12</sup> Marjan M. Weiss,<sup>10</sup> Stephanie Efthymiou,<sup>8</sup> Michael G. Hanna,<sup>8</sup> Carlo Minetti,<sup>13</sup> Pasquale Striano,<sup>13</sup> Livia Pisciotta,<sup>14</sup> Elisa De Grandis,<sup>14</sup> Janine Altmüller,<sup>15</sup> Peter Nürnberg,<sup>15</sup> Holger Thiele,<sup>15</sup> Uluc Yis,<sup>16</sup> Tuncay Derya Okur,<sup>16</sup> Ayse Ipek Polat,<sup>16</sup> Nafise Amiri,<sup>17</sup> Mohammad Doosti,<sup>18</sup> Ehsan Ghayoor Karimani,<sup>18,19</sup> Mehran B. Toosi,<sup>20</sup> Gabriel Haddad,<sup>6,7</sup> Mert Karakaya,<sup>21</sup> Brunhilde Wirth,<sup>5,21</sup> Johanna M. van Hagen,<sup>10</sup> Nicole I. Wolf,<sup>22</sup> Reza Maroofian,<sup>19</sup> Henry Houlden,<sup>8</sup> Sebahattin Cirak,<sup>3,4,5,\*</sup> and Joseph G. Gleeson<sup>1,2,\*</sup>

ADP-ribosylation, the addition of poly-ADP ribose (PAR) onto proteins, is a response signal to cellular challenges, such as excitotoxicity or oxidative stress. This process is catalyzed by a group of enzymes referred to as poly(ADP-ribose) polymerases (PARPs). Because the accumulation of proteins with this modification results in cell death, its negative regulation restores cellular homeostasis: a process mediated by poly-ADP ribose glycohydrolases (PARGs) and ADP-ribosylhydrolase proteins (ARHs). Using linkage analysis and exome or genome sequencing, we identified recessive inactivating mutations in *ADPRHL2* in six families. Affected individuals exhibited a pediatric-onset neurodegenerative disorder with progressive brain atrophy, developmental regression, and seizures in association with periods of stress, such as infections. Loss of the *Drosophila* paralog *Parg* showed lethality in response to oxidative challenge that was rescued by human *ADPRHL2*, suggesting functional conservation. Pharmacological inhibition of PARP also rescued the phenotype, suggesting the possibility of postnatal treatment for this genetic condition.

ADP-ribosylation is a tightly regulated posttranslational modification of proteins involved in various essential physiological and pathological processes, including DNA repair, transcription, telomere function, and apoptosis.<sup>1–3</sup> The addition of poly-ADP-ribose (PAR) is mediated by a group of enzymes, referred to as poly(ADP-ribose) polymerases (PARPs), in response to cellular stressors, such as excitotoxicity or reactive oxygen species. PARylated proteins can subsequently initiate cellular stress response pathways. After resolution of the original insult, ADP-ribose polymers are rapidly removed.<sup>4,5</sup> Although PAR modification can protect the cell from death in the setting of cellular stress, excessive PAR accumulation or failure to reverse PAR modification can trigger a cell-death response cascade.<sup>6,7</sup>

Humans have two genes encoding specific PAR-degrading enzymes: *ADPRHL2* (MIM: 610624; Gene ID: 54936) and *PARG* (MIM: 603501). Both are capable of hydrolyzing the glycosidic bond between ADP-ribose moieties and are ubiquitously expressed.<sup>8,9</sup> *ADPRH* (MIM: 603081) and putatively *ADPRHL1* (MIM: 610620) encode proteins that can cleave mono-ADP-ribosylated residues and thus are not functionally redundant with *ADPRHL2* and *PARG*.<sup>8</sup> Studies of *in situ* hybridization have shown high *Adprhl2* expression in the developing mouse forebrain and that its expression remains high in the cerebellum, cortex, hippocampus, and olfactory bulb in early postnatal ages and persists into adulthood.<sup>10</sup> *Parg*<sup>−/−</sup> mice die embryonically as a result of PAR accumulation and cellular apoptosis.<sup>11</sup> There are no reports of *Adprhl2*<sup>−/−</sup> animals,

<sup>1</sup>Laboratory for Pediatric Brain Disease, Howard Hughes Medical Institute, University of California, San Diego, La Jolla, CA 92093, USA; <sup>2</sup>Rady Children's Institute for Genomic Medicine, Rady Children's Hospital, San Diego, CA 92123, USA; <sup>3</sup>Center for Molecular Medicine Cologne, Cologne, Germany; <sup>4</sup>Department of Pediatrics, University Hospital of Cologne, Cologne, Germany; <sup>5</sup>Center for Rare Diseases, Cologne 50937, Germany; <sup>6</sup>Department of Pediatrics, University of California, San Diego, La Jolla, CA 92093, USA; <sup>7</sup>Rady Children's Hospital, San Diego, CA, USA; <sup>8</sup>Department of Neuromuscular Diseases and Neurogenetics Laboratory, University College of London, London WC1E 6BT, UK; <sup>9</sup>Department of Pediatrics, United Arab Emirates University and Tawam Hospital, PO Box 15551, Al Ain, Abu Dhabi, UAE; <sup>10</sup>Amsterdam UMC, Vrije Universiteit Amsterdam, Department of Clinical Genetics, De Boelelaan 1117, Amsterdam, the Netherlands; <sup>11</sup>Division of Medical Genetics, Department of Medicine, University of California, San Diego, San Diego, CA 92093, USA; <sup>12</sup>Kastamonu University, Medical Faculty, 37150 Kastamonu, Turkey; <sup>13</sup>Pediatric Neurology and Muscular Diseases Unit, Istituto Giannina Gaslini, Department of Neurosciences, Rehabilitation, Ophthalmology, Genetics, and Maternal and Children's Sciences, University of Genoa, Genoa 16126, Italy; <sup>14</sup>Child Neuropsychiatry Unit, Istituto Giannina Gaslini, Department of Neurosciences, Rehabilitation, Ophthalmology, Genetics, and Maternal and Children's Sciences, University of Genoa, Genoa 16126, Italy; <sup>15</sup>Cologne Center for Genomics, University of Cologne, Cologne 50931, Germany; <sup>16</sup>Department of Pediatrics, Division of Child Neurology, Dokuz Eylül University School of Medicine, İzmir 35340, Turkey; <sup>17</sup>Targeted Drug Delivery Research Center, Pharmaceutical Technology Institute, University of Medical Sciences, Mashhad 15731, Iran; <sup>18</sup>Next Generation Genetic Clinic, Mashhad 15731, Iran; <sup>19</sup>Molecular and Clinical Sciences Institute, St. George's, University of London, Cranmer Terrace, London SW17 0RE, UK; <sup>20</sup>Pediatric Neurology, Department of Pediatric Diseases, Faculty of Medicine, Mashhad University of Medical Sciences, Mashhad 15731, Iran; <sup>21</sup>Institute of Human Genetics, Center for Molecular Medicine, and Center for Rare Diseases, University of Cologne, Cologne 50937, Germany; <sup>22</sup>Department of Child Neurology, VU University Medical Center and Amsterdam Neuroscience, Amsterdam 1117, the Netherlands

\*Correspondence: sebahattin.cirak@uk-koeln.de (S.C.), jogleeson@ucsd.edu (J.G.G.)

<https://doi.org/10.1016/j.ajhg.2018.07.010>



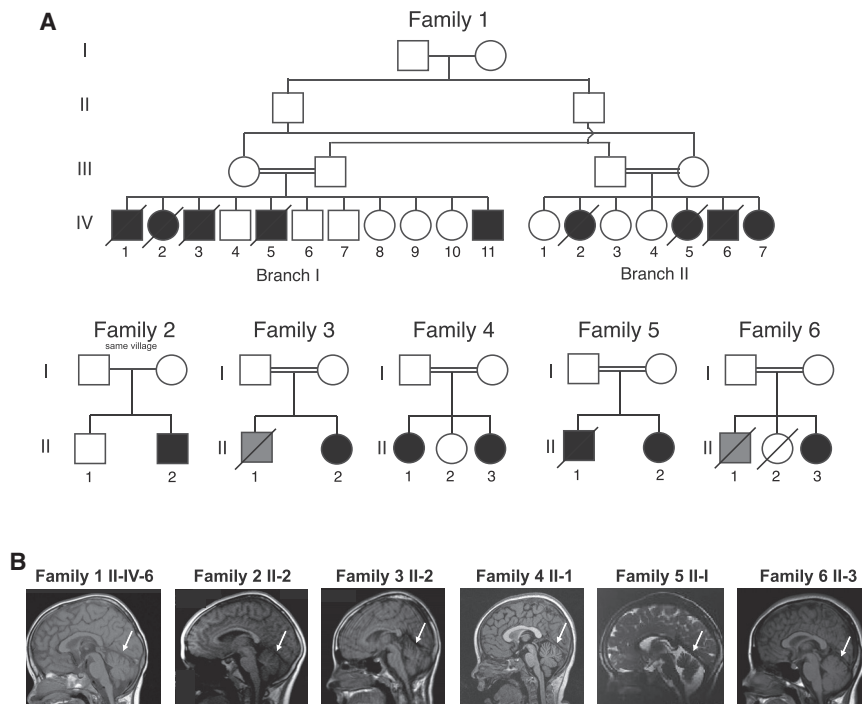


**Figure 1. Pedigrees of Families with Mutations in *ADPRHL2* and Their Clinical Presentation**

(A) Pedigrees of families 1–6 show consanguineous unions (double bar) and a total of 16 affected individuals. Slashes represent deceased individuals. Black shading indicates affected individuals. Gray shading indicates individuals who passed away from SUDEP; however, no DNA is available.

(B) Panels show midline sagittal MRI for one affected individual from each of the six families. White arrows indicate cerebellar atrophy, evidenced by widely spaced cerebellar folia.

able progression with developmental delay, intellectual disability, mild cerebellar atrophy (Figure 1B), and recurring seizures.

Genome-wide linkage analysis of 14 members of family 1 mapped the disease locus to an 11 Mb locus in chromosomal region 1p36 with a genome-wide-significant multipoint

LOD score of 3.4 (Figure S1A). Exome sequencing of individual II-IV-6 at >30× read depth for 96.9% of the exome revealed a single rare (allele frequency < 1:1,000) potentially deleterious variant within the linkage interval: a frameshift *ADPRHL2* mutation that segregated with the phenotype according to a recessive mode of inheritance.

Using GeneMatcher, this international collaborative group of authors identified further pathogenic alleles in *ADPRHL2*.<sup>17</sup> After obtaining informed consent from all participating individuals in accordance with the ethical standards of the responsible committee on human experimentation at the University of California, San Diego, we identified a total of six distinct mutations in ADP-ribosylhydrolase-like 2 (*ADPRHL2* [Gene ID: 54936]) in the six families by whole-exome or genome sequencing (see Supplemental Data). All variants were prioritized by allele frequency, conservation, blocks of homozygosity, and predicted effect on protein function (see Supplemental Data), and in all families the homozygous variant in *ADPRHL2* was the top candidate. Variants were confirmed by Sanger sequencing and segregated with the phenotype according to a recessive mode of inheritance. All variants were predicted to be disease causing by MutationTaster.<sup>18</sup> These variants were not encountered in dbGaP, the ExAC Browser, 1000 Genomes, genomAD, or the Greater Middle East Variome.

*ADPRHL2* contains six coding exons, yielding a single protein-coding transcript, ADP-ribosylhydrolase 3 (ARH3) (Figure 2A). The encoded 363 amino acid ARH3 is predicted to have a mitochondrial localization sequence and single enzymatic ADP-ribosyl-glycohydrolase domain (Figure 2B). Family 1 carried the homozygous exon 6 mutation c.1000C>T (GenBank: NM\_017825), which

but *Adprhl2*<sup>-/-</sup> mouse embryonic fibroblasts (MEFs) engineered to express the catalytic domain of nuclear PARP1 in mitochondria show PAR accumulation, as well as longer mitochondrial PAR polymers.<sup>12,13</sup>

*Drosophila melanogaster* has a single *Parg*-like gene, and null flies are lethal in the larval stage; however, when grown at a permissive temperature, a few can survive. The surviving flies display PAR accumulation, neurodegeneration, reduced locomotion, and premature death,<sup>14</sup> suggesting increased neuronal vulnerability to PAR accumulation. Although mutations in enzymes PARG and PARP have not been reported in human disease, other members of this pathway have been implicated in human phenotypes.<sup>15</sup> For example, mutations in *XRCC1* (MIM: 194360), encoding a molecular scaffold protein involved in complex assembly during the repair of DNA-strand breaks, lead to PARP-1 overactivation and are associated with cerebellar ataxia, ocular motor apraxia, and axonal neuropathy.<sup>16</sup>

In this study, we show that mutations in *ADPRHL2* underlie an age-dependent recessive epilepsy-ataxia syndrome initiating with sudden severe seizures in otherwise healthy individuals followed by progressive loss of milestones, brain atrophy, and death in childhood. We describe six independent families carrying *ADPRHL2* mutations leading to a nearly identical epilepsy-ataxia syndrome (Figure 1A). One of the six families (family 2) lacked documentation of parental consanguinity, and the parents from this family were from the same small village. The clinical details of subjects from all included families are shown in Table 1, and detailed clinical history is narrated in the Supplemental Note. The emerging clinical picture is one of a stress-induced neurodegenerative disease of vari-

introduces a premature stop codon (p.Gln334Ter) predicted to truncate the highly conserved last 30 amino acids of the protein, including part of the ADP-ribosylhydrolase domain. Family 2 harbored the homozygous exon 3 mutation c.316C>T (GenBank: NM\_017825), which also introduces a premature stop codon (p.Gln106Ter) in the ADP-ribosylhydrolase domain. Family 3 revealed the homozygous exon 2 missense mutation c.235A>C (GenBank: NM\_017825), which leads to an amino acid change (p.Thr97Pro) in a residue that is highly conserved among vertebrates (Figure S2A). Using a previously published crystal structure of ARH3, we localized this residue to an  $\alpha$ -helical loop within the ADP-ribosylhydrolase domain and the substrate binding site, which is defined by the position of two Mg<sup>2+</sup> ions located in adjacent binding sites; thus, the residue is predicted to affect protein structure and enzymatic activity (Figure S2B).<sup>19</sup> Family 4 carried the homozygous 5 bp, exon 3 deletion c.414\_418TGCCC (GenBank: NM\_017825), which results in a frameshift (p.Ala139GlyfsTer5) in the ADP-ribosylhydrolase domain. Family 5 carried the homozygous exon 4 missense mutation c.530C>T (GenBank: NM\_017825), which leads to an amino acid change (p.Ser177Leu) that is also highly conserved among vertebrates. It is localized in a critical  $\alpha$ -helical loop within the ADP-ribosylhydrolase domain, also suggesting an effect on protein structure and activity. Family 6 carried the homozygous exon 1 missense mutation c.100G>A (GenBank: NM\_017825), which leads to an amino acid change (p.Asp34Asn) that is highly conserved among vertebrates. This change is also localized in a critical  $\alpha$ -helical loop within the ADP-ribosylhydrolase domain, suggesting a potential impact on protein structure and activity.

The emerging phenotype of recessive *ADPRHL2* mutations is a degenerative pediatric-onset stress-induced epileptic-ataxia syndrome. Individuals with mutations in this gene are asymptomatic early after birth but gradually develop a cyclic pattern of illness-related spontaneous epileptic seizures or present with a neurodegenerative course including weakness, ataxia, and loss of milestones followed by clinical deterioration that ultimately leads to premature death. Most of the subjects succumbed to sudden unexpected death in epilepsy (SUDEP) or an apnoic-attack-like clinical presentation, suggesting a hyperacute presentation prior to the family's recognition of a predisposition. We could not establish an obvious genotype-phenotype correlation given that we show below that the missense mutation also leads to a severe loss of function. Thus, the clinical variability in the age of onset might occur because the genetic background or environmental challenges lead to variable susceptibility to illness-related cellular stress.

The differential diagnosis for this condition was based upon the presentation of a recessive condition with recurrent exacerbations and predominant features of global developmental delay, intellectual disability, seizures, neurogenic changes on electromyography, hearing impair-

ment, regression, and mild cerebellar atrophy but not microcephaly or cataracts. The differential diagnosis in our families included mitochondrial disorders, spastic ataxia, and peripheral neuropathy.

To determine the impact of these mutations on protein folding and binding activity, we generated recombinant proteins in *E.coli* and purified them by His-tag affinity chromatography. Our results showed that the p.Gln334Ter protein was not evident in the soluble fraction, whereas the wild-type (WT) was recovered with good purity (Figure S3A). The p.Thr79Pro protein was expressed and soluble, although possibly recovered with slightly less purity than WT ARH3. We studied the deleterious impact of p.Thr79Pro by using circular dichroism spectroscopy (Figures S3B and S3C). Compared with the WT, this mutant exhibited reduced  $\alpha$ -helical content and an altered secondary structure, in agreement with the fact that p.Thr79Pro occurred within an  $\alpha$ -helical domain. Further, the melting temperature ( $T_m$ ) of p.Thr79Pro was reduced by more than 10°C, confirming destabilization of the mutant (Figures S3D–S3F). We also found that in contrast to WT ARH3, the p.Thr79Pro protein was not stabilized by ligands such as adenosine diphosphate ribose (ADPr) (Figures S3G–S3I). We confirmed the specificity of this assay by using adenosine triphosphate (ATP) and ribose-5-phosphate as negative controls, which were not predicted to bind or stabilize ARH3. Together, these data suggest that both disease-causing, truncating mutants and amino acid substitutions should be destabilized when expressed in cells.

Because the c.1000C>T (p.Gln334ter) mutation of family 1 was in the last exon, we first excluded nonsense-mediated decay (NMD) of the mutant mRNA. We collected skin biopsies from the father (III-II) and two affected individuals (II-IV-6 and II-IV-7), generated primary fibroblasts, and then performed RT-PCR by using primers designed to amplify the last three exons of *ADPRHL2* (Figure S1B). The father's and affected individuals' cells revealed a band of the expected size and of similar intensity to that of a healthy control individual, arguing against NMD. However, when we used an antibody recognizing amino acids 231–245, lysates derived from the affected individuals showed no detectable ARH3 (Figure 2C; Supplemental Data), consistent with a null effect of the truncating mutation. Further, western blot analysis of individual II-2 from family 2 showed an absence of the protein, as predicted by the early stop codon. Fibroblasts from individual II-1 from family 3 showed a severely reduced amount of ARH3 (Figure 2C), consistent with the thermal instability of this mutant protein (Figures S3D–S3F) and the severe alteration of its secondary structure (Figures S3B and S3C).

Whereas humans have two known genes with specific PARG activity (*PARG* and *ADPRHL2*; Figure 3A), *Drosophila* have a single gene that regulates this process: *Parg*. Using the Gal4-UAS system to drive RNAi expression, we found that *Parg* knockdown led to a 60% decrease in total *Parg* mRNA for flies with the ubiquitous *da* promoter and a

**Table 1. Mutations in ADPRHL2 Cause Various Phenotypes, Including Developmental Delay, Cerebellar Atrophy, Ataxia, and Epilepsy**

<b>Family 1</b>								
	<b>I-IV-1</b>	<b>I-IV-2</b>	<b>I-IV-3</b>	<b>I-IV-5</b>	<b>I-IV-11</b>	<b>II-IV-2</b>	<b>II-IV-5</b>	<b>II-IV-6 (A1)</b>
Gender	M	F	M	M	M	F	F	M
Country of origin	UAE	UAE	UAE	UAE	UAE	UAE	UAE	UAE
Parental consanguinity	+	+	+	+	+	+	+	+
Current age or age of death	died at 4 years	died at 2 years	died at 7 years	died at 15 years	4 years	died at 2 years	died at 2 years	died at 9 years
Circumstances of death	in sleep	in sleep	seizure	respiratory failure	–	in sleep 1 week after flu-like illness	seizure after playing	respiratory failure after long airplane trip
<b>Mutation</b>								
Genomic (hg19 <sup>a</sup> )	g.36558895C>T	g.36558895C>T	g.36558895C>T	g.36558895C>T	g.36558895C>T	g.36558895C>T	g.36558895C>T	g.36558895C>T
cDNA	c.1000C>T	c.1000C>T	c.1000C>T	c.1000C>T	c.1000C>T	c.1000C>T	c.1000C>T	c.1000C>T
Protein	p.Gln334*	p.Gln334*	p.Gln334*	p.Gln334*	p.Gln334*	p.Gln334*	p.Gln334*	p.Gln334*
Homozygosity	+	+	+	+	+	+	+	+
<b>Perinatal History</b>								
Normal birth	+	+	+	+	+	+	+	+
Normal early development	+	+	+	+	+	+	+	+
<b>Psychomotor Development</b>								
Speech development	spoke in sentences but then deteriorated	few words at 2 years	normal until 2.5 years but then no further development	normal until 3.5 years but then deteriorated	speaks only a few words	normal speech until death	normal speech until death	normal until 25 years but then deteriorated
Motor development	normal but then deteriorated	normal until death	normal but then deteriorated	normal but then deteriorated	normal but then deteriorated	normal but then deteriorated	normal until death	normal but then deteriorated by 2 years
<b>Seizures</b>								
Seizure onset	18 months	19 months	19 months	24 months	15 months	24 months	15 months	18 months
Seizure types	GTCS	GTCS	GTCS	GTCS	absence, GTCS	GTCS	GTCS	absence, GTCS
<b>Neurological Examination</b>								
Intellect	normal but then delayed	normal until death	normal but then delayed	normal but then delayed	normal but then delayed	normal until death	normal until death	normal but then delayed
EEG	–	–	–	–	–	–	–	generalized epileptiform activity, slow background
MRI (age performed)	–	–	–	normal (5 years)	–	–	–	mild cerebellar atrophy (7 years)

*(Continued on next page)*

	Family 2	Family 3	Family 4		Family 5		Family 6
II-IV-7 (A2)	II-2	II-1	II-1	II-3	IV-1	IV-2	II-3
F	M	F	F	F	M	F	F
UAE	Italy	Turkey	Pakistan	Pakistan	Iran	Iran	Turkey
+	same village	+	+	+	+	+	+
3 years	16 years	15 years	13 years	2 years	died at 6 years	3 years	10 years
-	-	-	-	-	in sleep	-	-
g.36558895C>T	g.36557226C>T	g.36556868A>C	g.36557324_36557328delTGCCC	g.36557324_36557328delTGCCC	g.36557524C>T	g.36557524C>T	g.36554605G>A
c.1000C>T	c.316C>T	c.235A>C	c.414_418delTGCCC	c.414_418delTGCCC	c.530C>T	c.530C>T	c.100G>A
p.Gln334*	p.Gln106*	p.Thr79Pro	p.Ala139Glyfs*4	p.Ala139Glyfs*4	p.Ser177Leu	p.Ser177Leu	p.Asp34Asn
+	+	+	+	+	+	+	+
+	+	+	+	+	+	+	+
+	+	+	+	mild developmental delay	+	+	+
normal speech but then deteriorated	slow speech	normal	normal	delayed	normal until 1.5 years but then deteriorated with difficulty speaking	speaks only a few words	delayed
walked normally at 14 months but then had ataxia and poor balance at 19 months	normal but then deteriorated by 2 years	normal	normal but then deteriorated by 2 years	mildly delayed	normal until 1 year but then deteriorated	normal but then deteriorated by 1.5 years	normal
16 months	-	-	-	9 months	24 months	36 months	-
absence, GTCS	-	-	GTCS with illness	GTCS with illness	multifocal, GTCS	multifocal, GTCS	-
normal but then delayed	normal but then started deteriorating at age 11 years	normal	mild ID (IQ 60)	mild global developmental delay	normal but then stagnated	normal but then stagnated	mild ID
generalized epileptiform activity, slow background	-	-	mild slowing background activity (3 years)	normal	generalized epileptiform activity, slow background	normal	normal
mild cerebellar atrophy (7 years)	cerebellar vermis atrophy (11 years)	mild cerebellar atrophy, spinal cord atrophy (12 years)	mild cerebellar atrophy (4 years)	normal (11 months)	-	normal (3 years)	mild cerebellar vermis atrophy, spinal cord atrophy (15 years)

(Continued on next page)

**Table 1. Continued**

	Family 1							
	I-IV-1	I-IV-2	I-IV-3	I-IV-5	I-IV-11	II-IV-2	II-IV-5	II-IV-6 (A1)
EMG or biopsy	-	-	-	-	-	-	-	nerve biopsy with severe axonal loss
Onset of unsteady gait	-	-	2.5 years	3 years	2.5 years	-	-	2.5 years
<b>Other Clinical Features</b>								
Exacerbated by illness and/or stress	+	+	+	+	+	+	+	+
Other clinical features	-	-	-	hypotonia with repeated pneumonia, ventilator dependent at time of death	can walk but is very unsteady	progressive weakness	progressive weakness	repeated pneumonia, repeated cardiac arrest, profound type II muscle fiber atrophy

Clinical presentation for affected subjects from families 1–6. Abbreviations are as follows: +, yes; -, not available; DTR, deep-tendon reflex; EEG, electroencephalography; EMG, electromyography; F, female; GTCS, generalized tonic-clonic seizure; ID, intellectual disability; M, male; MRI, magnetic resonance imaging; and SNHL, sensorineural hearing loss.  
<sup>a</sup>UCSC Genome Browser.

50% decrease with the neuron-specific promoter, *elav* (*embryonic lethal abnormal visual system*) (Figure S4A). Whereas the *da-Gal4* and *Parg*<sup>RNAi</sup> lines showed normal survival, crossing the two together led to *daughterless* (*da*)-mediated expression of *Parg*<sup>RNAi</sup>, which reduced survival substantially (Figure S4B). Ubiquitous knockdown of *Parg* also led to decreased survival when animals were exposed to stress with either hydrogen peroxide (H<sub>2</sub>O<sub>2</sub>) in their water or environmental hypoxia (2% O<sub>2</sub>) (Figures S4C and S4D). Furthermore, knockdown of *Parg* specifically in neurons largely recapitulated this phenotype by using the same two environmental stressors (Figures S4E and S4F). These data provide evidence that stress leads to premature death in the absence of *Parg* and that neurons play an important role in this phenotype.

However, lethality of these flies was not as severe as in the *Parg*<sup>27.1</sup> line, which carries a p-element insertion that deletes two-thirds of the open reading frame (nucleotides 34,622–36,079 of GenBank: Z98254),<sup>14</sup> suggesting that *Parg*<sup>RNAi</sup> is partially inactivating. These mutant flies with *Parg* loss of function lack the protein Parg and show elevated amounts of PAR, especially in nervous tissue.<sup>14</sup> Mutant flies die in larval stages, but 25% of the animals survive when grown at the permissive 29°C temperature. These adult flies display progressive neurodegeneration, reduced locomotion, and reduced lifespan,<sup>14</sup> consistent with the individuals' phenotypes in our families. We confirmed lethality of the *Parg*<sup>27.1</sup> line and found that forced expression of *Drosophila Parg* under the ubiquitous *da* promoter in the mutant background increased both survival and motor activity as measured by an established "climbing index" (Figures 3B and 3C).<sup>20</sup> Likewise, expression of the human *ADPRHL2* under the same *da* promoter

showed a nearly identical degree of rescue of both survival and locomotor activity (Figures 3B and 3C). These results suggest that human *ADPRHL2* is a functional paralog of *Drosophila Parg*.

We next tested whether this phenotype might be ameliorated by inhibition of protein PARylation. We reasoned that the requirement for dePARylation should be reduced by the blockage of stress-induced PARylation. Minocycline displays PARP inhibitory activity with an IC<sub>50</sub> of 42 nM in humans<sup>21</sup> and is well tolerated in flies.<sup>22</sup> We fed flies with a range of concentrations from 0 to 1 mg/mL minocycline for 24 hr before stress and measured survival rates 96 hr after stress induction. Drug treatment of flies with ubiquitous knockdown of *Parg* revealed a dose-dependent partial rescue of the lethality (Figure S4G). This rescue was also seen when the drug was given to flies with neuron-specific knockdown of *Parg* (Figure S4H), providing evidence that PARP inhibition can rescue lethality *in vivo*. Although we expect that the effect of minocycline on survival in this assay was due to its effect on PARP, we cannot exclude off-target or non-specific effects.<sup>22</sup>

Given that PARP inhibitors are currently in trials for various types of cancer, it is possible that these drugs could be tested for clinical effectiveness in this orphan disease, where they could have a positive effect. Potentially clinically relevant PARP inhibitors include (1) minocycline, an FDA-approved tetracycline derivative that displays PARP inhibitory activity; (2) dihydroisoquinoline (DPQ), a non-FDA-approved potent PARP-1 inhibitor used in experimental research; and (3) veliparib (ABT: 888), a potent PARP-1 and PARP-2 inhibitor currently in clinical trials for the treatment of various type of cancers (IC<sub>50</sub> = 42, 37, and 4.4 nM, respectively).<sup>21,23</sup>

	Family 2	Family 3	Family 4		Family 5	Family 6	
II-IV-7 (A2)	II-2	II-1	II-1	II-3	IV-1	IV-2	II-3
-	-	axonal polyneuropathy (4 years)	normal muscle biopsy (4 years)	-	normal (4 years)	axonal polyneuropathy (4 years)	axonal polyneuropathy
20 months	11 years	4 years	2.5 years	not yet	1.5 years	1.5 years	10 years
+	+	+	+	+	+	+	+
normal hearing but then developed severe SNHL, severe kyphoscoliosis, one episode of cardiac arrest	myopathic changes on muscle biopsy (11 years)	claw hand and pes cavus deformities, scoliosis, SNHL at 10 years, tracheotomy, ventilation	asthma	-	progressive weakness, tremors, frequent falling	progressive weakness, progressive external ophthalmoplegia	distal muscle atrophy, pes cavus deformity, toe abnormality, scoliosis, brisk DTRs, positive Babinski reflex, intentional tremor, ataxia

The extent to which *ADPRHL2* and *PARG* functionally diverge or converge is not well understood, partly because of a lack of detailed comparative expression analysis and biochemical function. *PARG* demonstrates greater specific activity than *ARH3* for removing PAR from proteins,<sup>8</sup> and loss of *Parg* in mice is embryonically lethal.<sup>13</sup> Together, these data suggest that *PARG* is likely to be the major contributor to PAR removal in cells that express both genes under basal conditions. One possibility is that *ADPRHL2*

acts as a backup for *PARG* to remove excessive PAR moieties under stress conditions. This would be consistent with the clinical presentation of individuals with loss of *ADPRHL2*, where phenotypes appear to be induced by environmental stress. Recent studies have shown that *ARH3* acts on a recently discovered form of Ser-ADP ribosylation.<sup>24</sup> For example, studies have illustrated an excessive accumulation of Ser-poly-ADP-ribosylated enzymes in *ADPRHL2*<sup>-/-</sup> cell lines and that *ARH3* acts mainly on

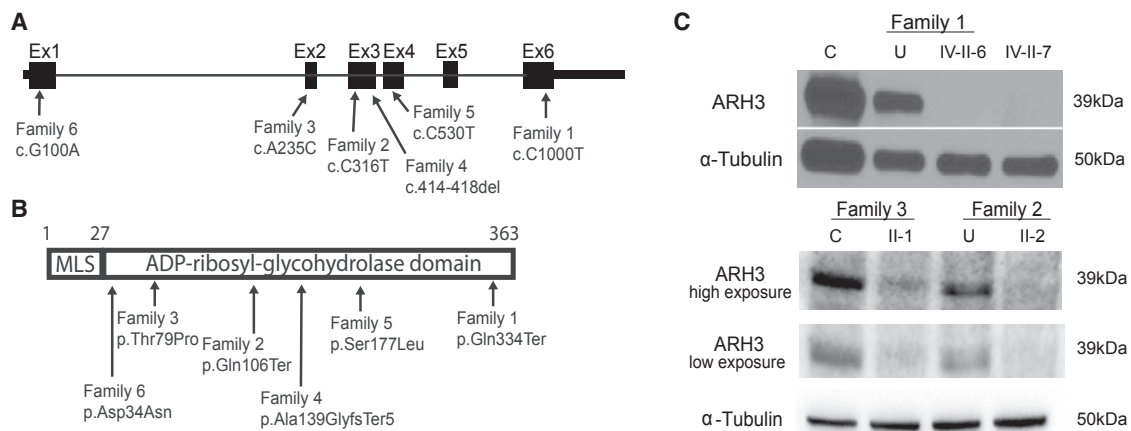


**Figure 2. Truncating and Missense *ADPRHL2* Mutations in Six Independent Families Are Predicted to Be Inactivating**

(A) Schematic of *ADPRHL2* depicts the coding sequence spanning six exons and the 5' and 3' UTRs. Black arrows indicate the positions of the six identified mutations and their coordinates within the cDNA (Gene ID: 54936).

(B) Schematic of *ARH3* depicts the mitochondrial localization sequence (MLS) and the ADP-ribosyl-glycohydrolase domain. Black arrows indicate the position and coordinates of the impact of the described mutations.

(C) Western blot of fibroblasts from an unrelated control individual (C), the unaffected carrier father (U), and affected individuals IV-II-6 and IV-II-7 from family 1 shows the absence of *ARH3* in affected fibroblasts.  $\alpha$ -tubulin was used as the loading control. Western blot of fibroblasts from an unrelated control individual (C) and affected individual II-1 from family 3 and the unaffected carrier mother (U) and affected individual II-3 from family 2 shows significantly reduced amounts of *ARH3*.  $\alpha$ -tubulin was used as the loading control.

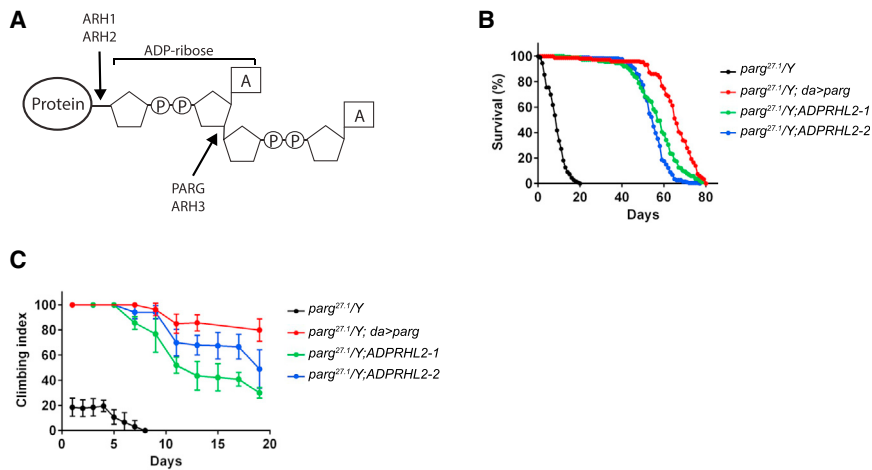


**Figure 3. Premature Death and Locomotor Defects in *Drosophila Parg* Mutants Are Rescued by Human *ADPRHL2***

(A) Schematic of a poly-ADP-ribosylated protein and the location of cleavage. *PARG* and *ADPRHL2* both remove poly-ADP-ribose (PAR) from proteins and cleave the same site. *Drosophila melanogaster* has one PAR-removing enzyme, *Parg*.

(B) *Parg*<sup>27.1</sup> mutant flies (black) show a severe climbing defect, which was rescued by ubiquitous forced expression of *Parg* (red) or mis-expression of human *ADPRHL2* in two different transgenic lines (green and blue).

(C) *Parg*<sup>27.1</sup> mutant flies (black) displayed decreased survival, which was rescued with ubiquitous forced expression of *Parg* (red) and two different transgenic lines expressing human *ADPRHL2* (green and blue). Data represent the mean  $\pm$  SEM of eight experiments.

Ser-ADPr removal.<sup>25</sup> This would be consistent with the phenotype we see in subjects with loss of ARH3, where phenotypes do not emerge until environmental stress insults are encountered. Finally, ARH3 contains a mitochondrial localization signal, and thus another possibility is that ARH3 functions as a mitochondrial-specific glycohydrolase that is required after the induction of oxidative stress.<sup>13</sup>

PAR signaling has been shown to play a role in a number of cellular processes—including the regulation of transcription, telomere function, mitotic spindle formation, intracellular trafficking, and energy metabolism—in addition to apoptosis-inducing-factor (AIF)-mediated apoptosis.<sup>2,3</sup> Although we hypothesize that the disease mechanism is through cell death, it is possible that PAR accumulation could affect other cellular processes before this. Further work is needed to characterize these effects in the context of this disease.

### Accession Numbers

The exome sequencing data from individuals from the University of California, San Diego, study site have been deposited in the Database of Genotypes and Phenotypes under accession number dbGaP: phs000288.v1.

### Supplemental Data

Supplemental Data include a Supplemental Note, Supplemental Material and Methods, four figures, and one table and can be found with this article online at <https://doi.org/10.1016/j.ajhg.2018.07.010>.

### Acknowledgments

The authors thank the subjects and their families for participating in this study. S.G. was sponsored by the Ruth L. Kirschstein Institutional National Research Service Award (T32 GM008666) from the National Institute on Deafness and Other Communica-

tion Disorders and by award F31HD095602 from the NIH Eunice Kennedy Shriver National Institute of Child Health and Human Development. We thank the Broad Institute (U54HG003067 to E. Lander and UM1HG008900 to D. MacArthur) and the Yale Center for Mendelian Disorders (U54HG006504 to R. Lifton and M. Gunel). We also thank Lisa Weixler for technical assistance and all the staff of the Cologne Center for Genomics for next-generation sequencing. The sequencing data were analyzed with the CHEOPS high-performance computer cluster of the Regional Computing Center of the University of Cologne. We thank DeCode for whole-genome sequencing. This work was supported by NIH grants R01NS048453 and R01NS052455, the Simons Foundation Autism Research Initiative, the Howard Hughes Medical Institute (to J.G.G.), the Deutsche Forschungsgemeinschaft Emmy Noether Programme (grant CI 218/1-1 to S.C.), the Wellcome Trust (WT093205MA and WT104033AIA), Ataxia UK, the UCL/UCLH NIHR Biomedical Research Centre, the Medical Research Council (to H.H. and M.H), EU Horizon 2020 Solve-RD, and the European Community's Seventh Framework Programme (FP7/2007-2013) under grant 2012-305121 for the "Integrated European -omics research project for diagnosis and therapy in rare neuromuscular and neurodegenerative diseases (NEUROMICS)" to B.W.

### Declaration of Interests

The authors declare no competing interests.

Received: April 16, 2018

Accepted: July 15, 2018

Published: August 9, 2018

### Web Resources

1000 Genomes, <http://browser.1000genomes.org>

dbSNP, <http://www.ncbi.nlm.nih.gov/projects/SNP>

Exome Aggregation Consortium (ExAC) Browser, <http://exac.broadinstitute.org/>

dbGaP, <https://www.ncbi.nlm.nih.gov/gap>

FlyBase, <http://flybase.org>

GenBank, <https://www.ncbi.nlm.nih.gov/genbank/>  
 Gene, <https://www.ncbi.nlm.nih.gov/gene>  
 GeneMatcher, <https://genematcher.org>  
 HaplotypeCaller and GATK, <https://www.broadinstitute.org/gatk/>  
 Iranome, <http://www.iranome.ir/>  
 Mutation Assessor, <http://mutationassessor.org/>  
 MutationTaster, <http://mutationtaster.org/>  
 NHLBI Exome Sequencing Project Exome Variant Server, <http://evs.gs.washington.edu/EVS/>  
 OMIM, <http://omim.org/>  
 PolyPhen-2, <http://genetics.bwh.harvard.edu/pph2/>  
 Provean, <http://provean.jcvi.org>  
 RefSeq, <http://www.ncbi.nlm.nih.gov/RefSeq>  
 SIFT, <http://sift.jcvi.org/>  
 UniProt, <http://www.uniprot.org>

## References

- Hassa, P.O., Haenni, S.S., Elser, M., and Hottiger, M.O. (2006). Nuclear ADP-ribosylation reactions in mammalian cells: Where are we today and where are we going? *Microbiol. Mol. Biol. Rev.* *70*, 789–829.
- Luo, X., and Kraus, W.L. (2012). On PAR with PARP: Cellular stress signaling through poly(ADP-ribose) and PARP-1. *Genes Dev.* *26*, 417–432.
- Schreiber, V., Dantzer, F., Ame, J.C., and de Murcia, G. (2006). Poly(ADP-ribose): Novel functions for an old molecule. *Nat. Rev. Mol. Cell Biol.* *7*, 517–528.
- De Vos, M., Schreiber, V., and Dantzer, F. (2012). The diverse roles and clinical relevance of PARPs in DNA damage repair: Current state of the art. *Biochem. Pharmacol.* *84*, 137–146.
- Wang, Z., Wang, F., Tang, T., and Guo, C. (2012). The role of PARP1 in the DNA damage response and its application in tumor therapy. *Front. Med.* *6*, 156–164.
- Andrabi, S.A., Kim, N.S., Yu, S.W., Wang, H., Koh, D.W., Sasaki, M., Klaus, J.A., Otsuka, T., Zhang, Z., Koehler, R.C., et al. (2006). Poly(ADP-ribose) (PAR) polymer is a death signal. *Proc. Natl. Acad. Sci. USA* *103*, 18308–18313.
- Wang, Y., Dawson, V.L., and Dawson, T.M. (2009). Poly(ADP-ribose) signals to mitochondrial AIF: A key event in parthanatos. *Exp. Neurol.* *218*, 193–202.
- Oka, S., Kato, J., and Moss, J. (2006). Identification and characterization of a mammalian 39-kDa poly(ADP-ribose) glycohydrolase. *J. Biol. Chem.* *281*, 705–713.
- Poitras, M.F., Koh, D.W., Yu, S.W., Andrabi, S.A., Mandir, A.S., Poirier, G.G., Dawson, V.L., and Dawson, T.M. (2007). Spatial and functional relationship between poly(ADP-ribose) polymerase-1 and poly(ADP-ribose) glycohydrolase in the brain. *Neuroscience* *148*, 198–211.
- Magdaleno, S., Jensen, P., Brumwell, C.L., Seal, A., Lehman, K., Asbury, A., Cheung, T., Cornelius, T., Batten, D.M., Eden, C., et al. (2006). BGEM: An in situ hybridization database of gene expression in the embryonic and adult mouse nervous system. *PLoS Biol.* *4*, e86.
- Koh, D.W., Lawler, A.M., Poitras, M.F., Sasaki, M., Wattler, S., Nehls, M.C., Stöger, T., Poirier, G.G., Dawson, V.L., and Dawson, T.M. (2004). Failure to degrade poly(ADP-ribose) causes increased sensitivity to cytotoxicity and early embryonic lethality. *Proc. Natl. Acad. Sci. USA* *101*, 17699–17704.
- Niere, M., Kernstock, S., Koch-Nolte, F., and Ziegler, M. (2008). Functional localization of two poly(ADP-ribose)-degrading enzymes to the mitochondrial matrix. *Mol. Cell Biol.* *28*, 814–824.
- Niere, M., Mashimo, M., Agledal, L., Dölle, C., Kasamatsu, A., Kato, J., Moss, J., and Ziegler, M. (2012). ADP-ribosylhydrolase 3 (ARH3), not poly(ADP-ribose) glycohydrolase (PARG) isoforms, is responsible for degradation of mitochondrial matrix-associated poly(ADP-ribose). *J. Biol. Chem.* *287*, 16088–16102.
- Hanai, S., Kanai, M., Ohashi, S., Okamoto, K., Yamada, M., Takahashi, H., and Miwa, M. (2004). Loss of poly(ADP-ribose) glycohydrolase causes progressive neurodegeneration in *Drosophila melanogaster*. *Proc. Natl. Acad. Sci. USA* *101*, 82–86.
- Bütepage, M., Ecke, L., Verheugd, P., and Lüscher, B. (2015). Intracellular mono-ADP-riboseylation in signaling and disease. *Cells* *4*, 569–595.
- Hoch, N.C., Hanzlikova, H., Rulten, S.L., Tétreault, M., Komulainen, E., Ju, L., Hornyak, P., Zeng, Z., Gittens, W., Rey, S.A., et al.; Care4Rare Canada Consortium (2017). XRCC1 mutation is associated with PARP1 hyperactivation and cerebellar ataxia. *Nature* *541*, 87–91.
- Sobreira, N., Schiettecatte, F., Valle, D., and Hamosh, A. (2015). GeneMatcher: A matching tool for connecting investigators with an interest in the same gene. *Hum. Mutat.* *36*, 928–930.
- Schwarz, J.M., Rödelsperger, C., Schuelke, M., and Seelow, D. (2010). MutationTaster evaluates disease-causing potential of sequence alterations. *Nat. Methods* *7*, 575–576.
- Mueller-Dieckmann, C., Kernstock, S., Lisurek, M., von Kries, J.P., Haag, F., Weiss, M.S., and Koch-Nolte, F. (2006). The structure of human ADP-ribosylhydrolase 3 (ARH3) provides insights into the reversibility of protein ADP-riboseylation. *Proc. Natl. Acad. Sci. USA* *103*, 15026–15031.
- Madabattula, S.T., Strautman, J.C., Bysice, A.M., O’Sullivan, J.A., Androschuk, A., Rosenfelt, C., Doucet, K., Rouleau, G., and Bolduc, F. (2015). Quantitative analysis of climbing defects in a *Drosophila* model of neurodegenerative disorders. *J. Vis. Exp.* *100*, e52741.
- Alano, C.C., Kauppinen, T.M., Valls, A.V., and Swanson, R.A. (2006). Minocycline inhibits poly(ADP-ribose) polymerase-1 at nanomolar concentrations. *Proc. Natl. Acad. Sci. USA* *103*, 9685–9690.
- Lee, G.J., Lim, J.J., and Hyun, S. (2017). Minocycline treatment increases resistance to oxidative stress and extends lifespan in *Drosophila* via FOXO. *Oncotarget* *8*, 87878–87890.
- Donawho, C.K., Luo, Y., Luo, Y., Penning, T.D., Bauch, J.L., Bouska, J.J., Bontcheva-Diaz, V.D., Cox, B.F., DeWeese, T.L., Dillehay, L.E., et al. (2007). ABT-888, an orally active poly(ADP-ribose) polymerase inhibitor that potentiates DNA-damaging agents in preclinical tumor models. *Clin. Cancer Res.* *13*, 2728–2737.
- Fontana, P., Bonfiglio, J.J., Palazzo, L., Bartlett, E., Matic, I., and Ahel, I. (2017). Serine ADP-riboseylation reversal by the hydrolase ARH3. *eLife* *6*, e28533.
- Palazzo, L., Leidecker, O., Prokhorova, E., Dauben, H., Matic, I., and Ahel, I. (2018). Serine is the major residue for ADP-riboseylation upon DNA damage. *eLife* *7*, e34334.